google.org

RE<C: Brayton System Performance Summary

Introduction

Our design goal for the power conversion system of a CSP plant was to take an approach that was water-free, modular, and less expensive than steam-based CSP. This led us to examine the Brayton power cycle as a possible solution.

This document summarizes the key performance modeling related to Google's Brayton CSP project. More information on the design of the major equipment in Google's Brayton CSP system is available in the Brayton System Hardware Summary .

Performance Modeling

Static Design Point Models

Several computer models were created to help design the prototype engine and analyze its operating behavior over a range of steady state and dynamic operating conditions. Sets of key operating parameters, called design point models, were used to simulate the operating behavior of the engine. These parameters included pressures and temperatures at key points in the cycle, air mass flow rates, spool rotational speeds, and component efficiencies of the compressor, turbine, gearbox, and generator. In total, we used 23 independent design parameters and an equal number of nonlinear equations to define the relationship of the parameters with respect to each other. A feasible design solution is one in which all equations are satisfied with a set of key parameter values.

Solutions to this set of equations can only be found through iteration. Engine design models were built initially in a spreadsheet using ad-hoc iteration based on circular references, and

then later using a more robust Newton-Raphson iteration.[1] A more flexible Matlab model using Newton's method was also developed. The initial spreadsheet approach with circular references proved unreliable, but the Newton's method spreadsheet and Matlab models allowed for rapid and robust calculation over a wide range of design options.

Selecting the design point for the engine required optimization across multiple conflicting trade-offs and constraints. Considerations included pressure ratios, turbine inlet temperature, air mass flow, heat exchanger temperature limits, available turbomachinery, and many more. All of these factors affected aspects of the engine produced, including engine efficiency, operational stability, and cost. A sample trade study we developed is shown in the figure below. The figure shows the relationship between the temperatures at the two turbine inlets, the product of the two compressor pressure ratios, and the engine rated power. In this particular case, there was a design constraint that the low pressure turbine/compressor parameters were fixed (based on a commercially available turbocharger for a marine diesel engine).

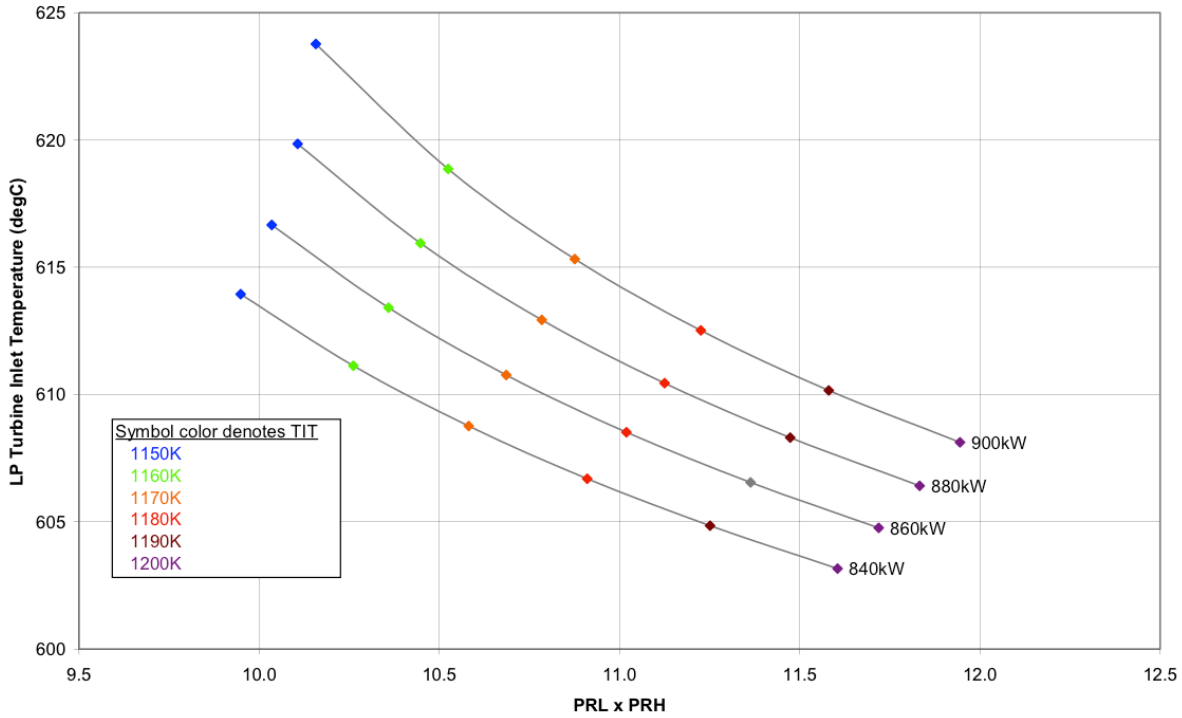

Example of design point trade-space. The graph shows feasible solutions given the constraint of using an off-the-shelf low pressure turbocharger. TIT is the high pressure turbine inlet temperature, and PRL x PRH is the product of the pressure ratios of the two compressor stages

Off-Design Dynamic Model

In addition to the design point models described above, a detailed dynamic performance model for the engine and receiver was also developed in Matlab. The design point models

[1] In numerical analysis, the Newton–Raphson method is a method for finding successively better approximations to the roots (or zeros) of a real-valued function.

were used first to determine the size and performance of the turbomachinery and heat exchangers at a desired design point. Then, detailed maps or models of the selected design point components operating at off-design conditions were generated based on adaptation of real world turbomachinery data. Interpolation of these maps is necessary in order to calculate component efficiencies and mass flows as functions of rotational speeds and pressure ratios.

The dynamic model calculates the system operating parameters over time, incorporating energy and momentum balances to simulate the dynamic response to changes in solar input and turbine nozzle position. The figure below shows one of the graphical output screens displaying key parameters as the code is running. The two compressor maps are on the left and the turbine maps are in the middle.

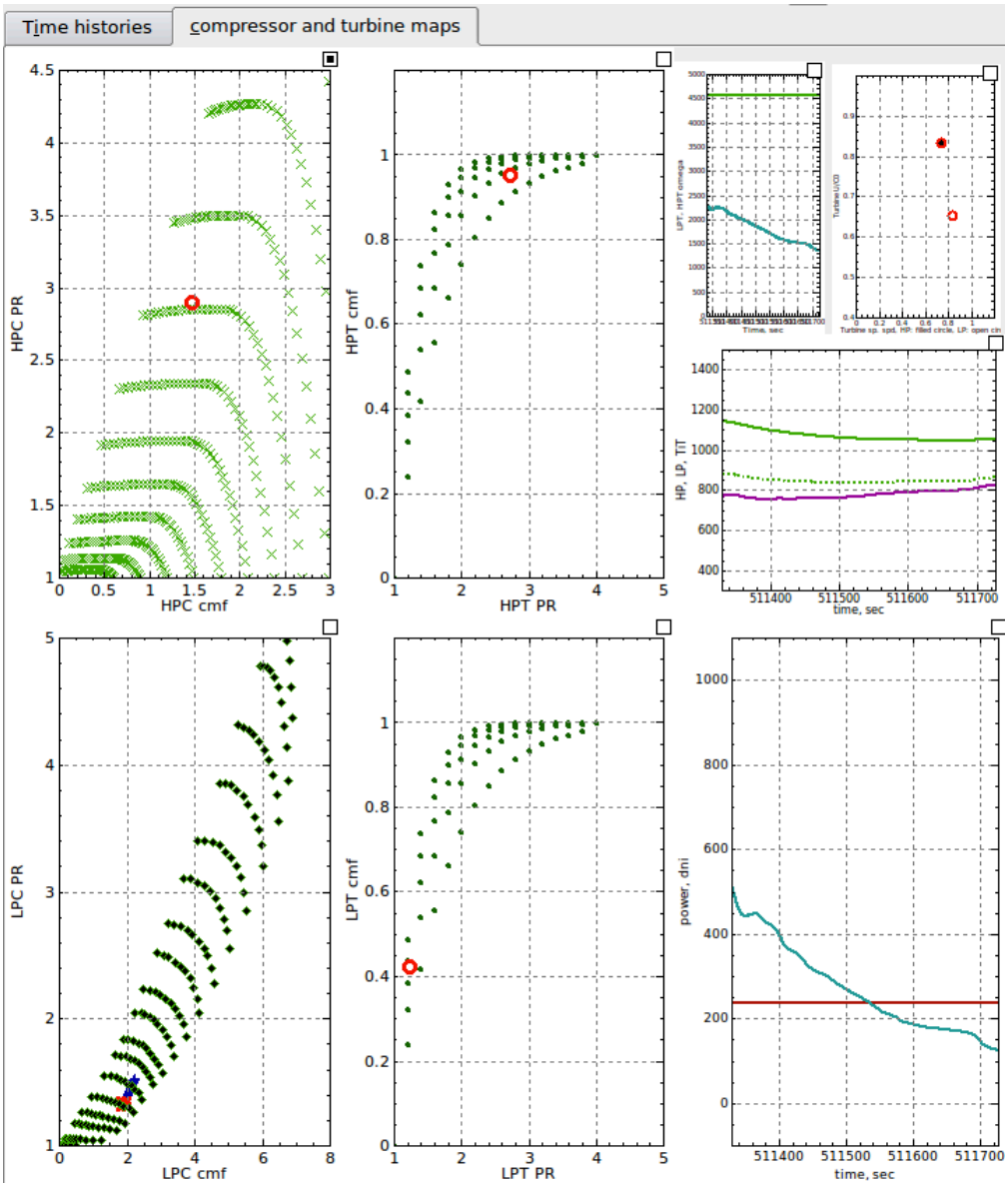

A snapshot in time of the off-design dynamic model output. The compressor maps are on the left (HP on top, LP on bottom), the turbine maps in the middle. The right column has shaft speeds at top left, turbine operating points on top right, key

temperatures in the middle, and engine power

Applications of the dynamic simulation model include:

- Validation of the design point and operation of the engine off-design (at different input power levels, ambient temperatures,etc.) to make sure the compressor stays on-map.
- Investigation of various nozzle control strategies.
- Dynamic response to sudden changes in direct normal insolation (DNI).[2]
- Engine capability for riding through long dropouts in DNI.
- Characterization of engine starting strategies and grid synchronization.
- Full-day engine simulations.

Receiver Efficiency Model

Once we determined the desired design points, the receiver design had two main challenges: feasibility and efficiency. Feasibility is addressed in the Brayton System Hardware Summary, and efficiency is addressed in the following sections.

An ideal receiver would transfer all of the light entering through the aperture into heating the compressed air inside. However, there are many sources of energy loss, making it challenging to achieve an acceptable thermal efficiency. For a given engine power output, higher receiver losses (and lower receiver efficiency) means building additional heliostats, and thus building a bigger (and more expensive) solar field. The bigger field would have a longer mean focal length, requiring a larger aperture to capture incoming solar flux, which in turn would increase the thermal losses. The causes and effects build on each other and can easily lead to spiralling out of a feasible design solution.

There are four major ways the receiver loses energy:

Reflection	Some of the light entering through the aperture ends up being reflected by internal surfaces (such as the back wall) and escapes back out through the aperture, either directly or after multiple bounces.
Radiation	Thermal radiation scales with surface temperature to the fourth power. It is kept in check by the cavity receiver design; much of the radiation from the hot surfaces inside the receiver falls back on other surfaces inside the receiver and is not lost.
Conduction	Heat is lost through conduction from the hot interior of the cavity through the cavity walls to the ambient temperature of the environment. Conduction losses can be limited to a reasonable total value by including sufficient insulation around the outside of the receiver; the ideal amount of insulation is driven by cost tradeoffs.
Convection	Convection losses involve movement of hot air from the inside of the

[2] Direct insolation is the solar irradiance measured at a given location on Earth with a surface element perpendicular to the Sun's rays.

receiver cavity to the outside environment. This can be either free convection (driven by the buoyancy of the hot air) or forced convection (driven by wind blowing across or into the cavity opening). Free convection losses in our design are minimized by designing the cavity aperture to point nearly straight down. With this "lookdown" aperture, hot air inside the cavity tends to stay inside the cavity.

The overall thermal efficiency of our receiver design is estimated to be 83%. The breakdown of the thermal power balance in the receiver is shown below.

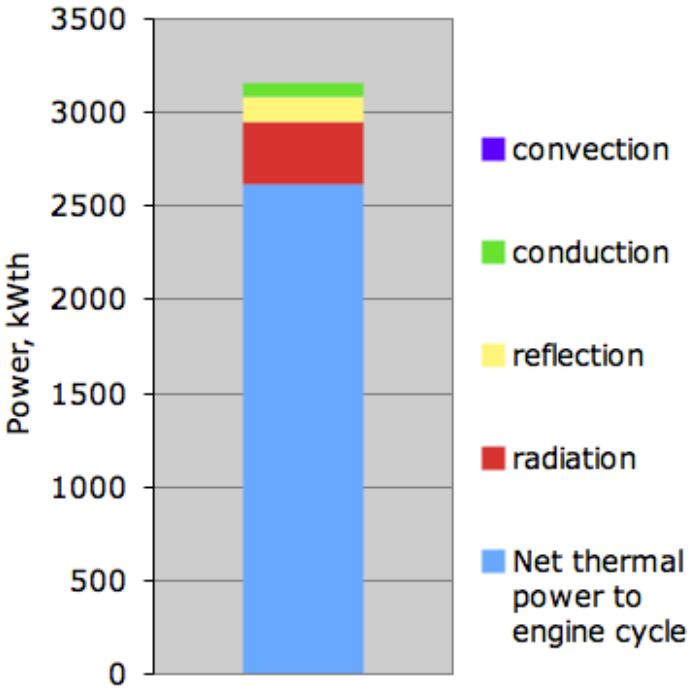

Breakdown of thermal power in the receiver (convection losses are assumed to be zero)

Engine Configuration and Design Point

The design point parameters for our prototype engine are shown in figure below. The power rating of 890 kW was chosen in order to use a large, off-the-shelf turbocharger for the low pressure spool.

Engine	
TIT HP (K)	1175
TIT LP (K)	883
Tamb (K)	298.2
Pamb (kPa)	93.8
PRL x PRH	10.95
massflow (kg/s)	4.828
LP power (shaft)	0.00
HP power (shaft)	949.8
Elec power (kW)	890.0

engine efficiency	33.96%

State Points	P (kPa)	T (K)
0	93.8	298.2
1	93.3	298.2
2	362.1	468.5
3	352.7	311.8
4	995.4	443.8
5	975.5	693.9
6	921.8	1175.0
7	234.6	882.7
8	234.6	882.7
9	96.9	721.7
10	94.3	473.1
11	93.8	473.1

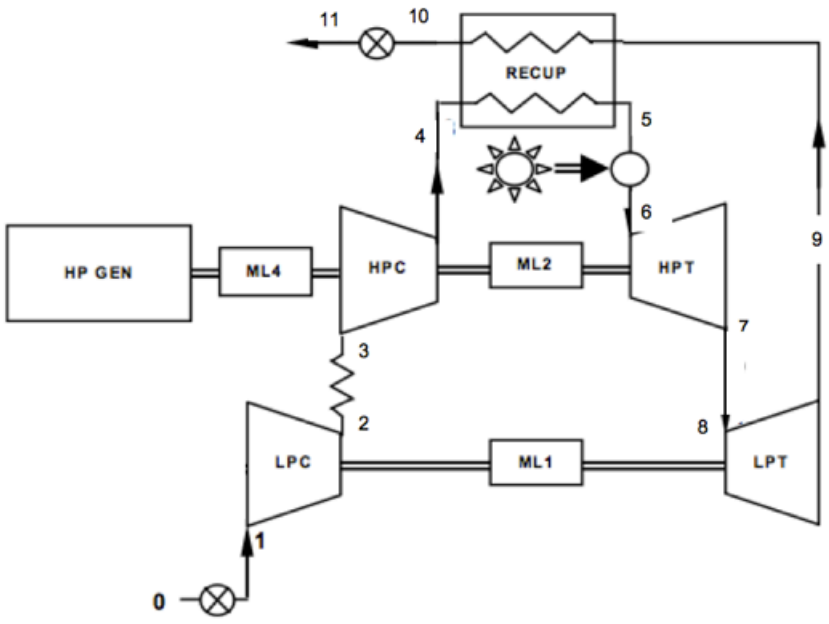

Final design point parameters

Results

Steady State Off-Design

The figure below shows how engine efficiency and overall system efficiency vary as a function of the design value of solar input power. Results are shown for four different ambient temperatures that cover the full range of expected operation (-3, 11, 25, and 42 deg C), as open-cycle Brayton engine efficiency can be strongly dependent on ambient temperature, and climates in areas with strong solar resources can be quite hot.

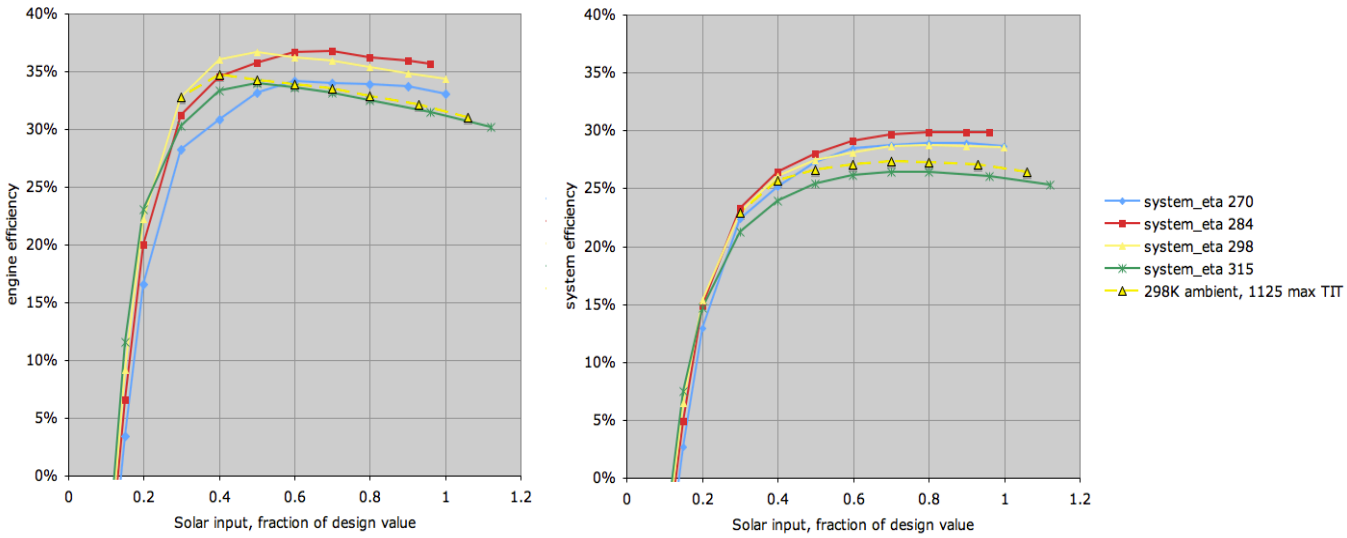

Engine and overall system efficiency as a function of fraction of rated solar input power. The different cases correspond to different ambient temperatures (given in Kelvin, converts to -3, 11, 25, and 42 deg C).

The next figure shows the turbine inlet temperature and nozzle positions for the off-design cases analyzed above. The target turbine inlet temperature is indicated as a dotted line on the upper graph. The target decreases at lower input power levels, in order to improve the overall system efficiency.

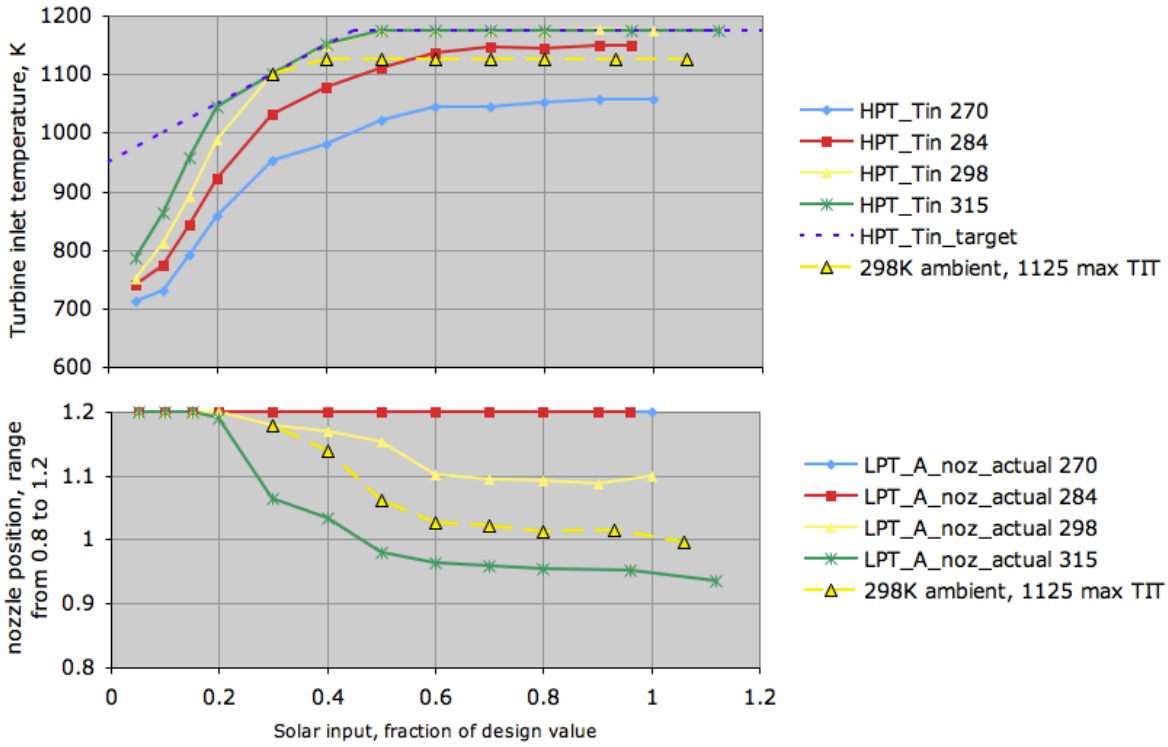

Turbine inlet temperature and nozzle positions.

Dynamic Response to Rapid Changes in Solar Input

The off-design dynamic model was used to model the dynamic response of the system to rapid changes in solar input. For example, a cloud passing the sun can bring direct normal insolation (DNI) down to zero W/m^2, cutting off all solar input into the system. Meanwhile, the solar receiver continues to lose energy through the same radiative, conductive, and convective losses described above, as well as through the continued extraction of energy by the working fluid stream. Not only does this reduction in operating temperature reduce the conversion efficiency of the engine, but it can also introduce an undesirable thermal cycle that reduces the life of the receiver through damage caused by rapid temperature changes and material fatigue.

The variable nozzles on the LP turbine allow for some control over the rate of energy extraction from the solar receiver by the working fluid (although they can't control for the other receiver thermal losses). Closing the nozzles from their nominal setting results in increased shaft power production by the LP turbine. This increased shaft power transfers to the LP compressor, which accelerates to a higher flow rate and higher pressure ratio operating point, and drives the engine to produce more power. Conversely, opening the nozzles results in a reduction of airflow through the engine and lower power output.

In order to avoid excessive thermal cycling of the solar receiver, one possible reaction to DNI dropouts would be to open the LP turbine nozzles and reduce the power output of the engine. This minimizes the rate of cooling of the receiver. It is important to keep all of the system parameters within their allowable operating envelopes, though, as opening the turbine nozzles too aggressively can cause the recuperator inlet temperature to exceed its maximum allowable temperature.

An example simulation showing this type of engine response to a 2-minute total dropout of solar input power is shown in the figure below.

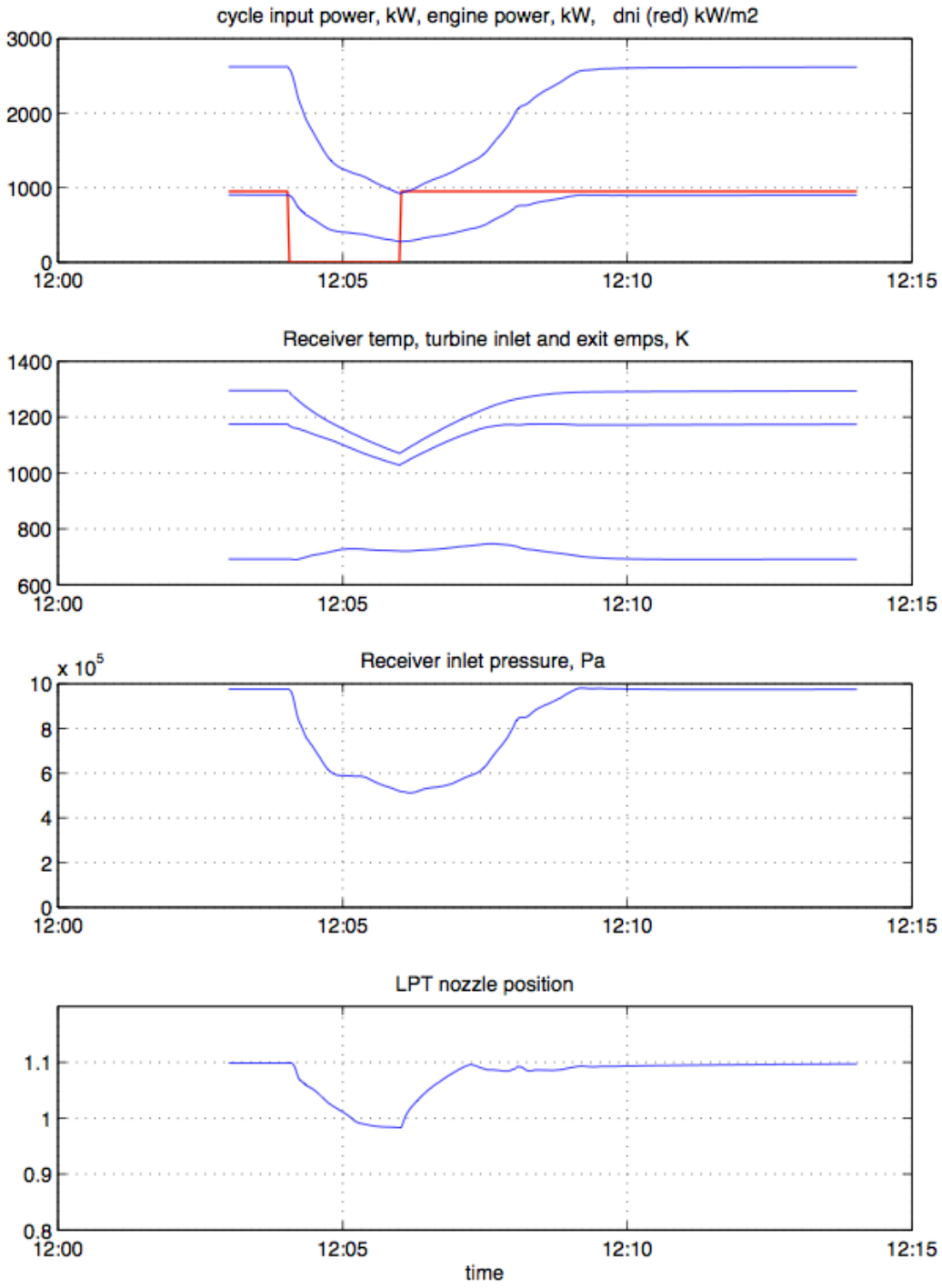

Time history traces for the 2-minute solar dropout (from 12:04 PM to 12:06 PM). This is a test case with a sharp-edged dropout of solar input.

Starting the Engine and Synchronizing With the Grid

A gas turbine with a synchronous generator must operate at a rotational speed that is locked on to the grid frequency. At some times, however, the generator can disconnect from the grid and

spin asynchronously. For solar Brayton engines, this generally occurs during engine startup or during extended cloud events.

In order to achieve synchronous operation, it is necessary to close a contactor that connects the generator to the grid. This has to be done very carefully; in order to avoid very large torque transients at the time of contactor closure, it is important to carefully match the voltage and phase of the generator terminals to those of the grid. A phase difference of less than 10 degrees (electrical) is a typical goal. Achieving this level of synchronization requires that the speed of the generator is controllable by some means near the synchronous speed.

Conventional fuel-fired gas turbine generators can achieve the speed control needed for synchronization through control of fuel flow. They use a motorized starter and fuel to start the engine up to a sub-synchronous idle speed. Then, with gradual addition of fuel, the speed can be brought up to synchronous speed, and the contactor can be closed when the measured phase error is within limits. This is similar to an electronic phase-lock loop.[3]

In a solar gas turbine, the heat input is not as controllable, which makes speed control based on solar "fuel" input difficult or impossible, given the heat capacity of the system and its interaction with the two stages of the engine configuration. If the engine starting procedure were attempted in a manner similar to that of a fuel-fired gas turbine, heat would be added to the receiver from a subset of the heliostat field, while a starter motor would gradually increase the speed of the HP stage. At some point, the starter motor torque would no longer be needed and the engine would be operating at idle with both spools free, meaning the high pressure (HP) spool would be disconnected from the grid at a sub-synchronous speed.

At first, the HP spool speed would rise gradually, along with the receiver temperature, but at some point the HP speed would begin to accelerate at an ever-increasing rate (i.e. positive jerk). The engine efficiency would increase as the pressure ratio rose, and the increased efficiency would result in more net torque available for acceleration of the spools. Further confounding the situation, the stored thermal energy in the receiver and recuperator would result in a temporary increase in the engine cycle input power as the engine air mass flow increased with speed. By the time the HP stage reached synchronous speed it would be accelerating at 1200 rpm/second. There is no realistic possibility of properly synchronizing the generator with the grid with this rate of acceleration.

As an alternative to the scenario outlined above, the following synchronization method was developed and tested in the dynamic engine simulation:

1. Apply solar heat to the solar receiver, either a normal morning solar ramp or a constant low value. Our simulation assumed a morning ramp.
2. Begin spinning up the HP stage with a variable frequency drive (VFD). Initially, the torque does not matter; it can be very low at low speed. At some moderate speed, apply constant torque (8 N-m at the spool). As the receiver temperature increases, the LP and HP spools will increase in speed.
3. Check the acceleration rate of HP spool. If acceleration rate multiplied by inertia exceeds the applied torque, the VFD won't have the authority to regulate speed, so abort the start.

[3] A phase-locked loop is a control system that generates an output signal whose phase is related to the phase of an input "reference" signal.

4. When the HP spool speed reaches nearly-synchronous speed (99.95% used in the example below), make a step-change reduction in the applied torque by an amount equal to the acceleration rate multiplied by the HP stage inertia. This will halt the acceleration temporarily.
5. Engage a simple proportional speed feedback loop targeting the nearly-synchronous speed target (again, 99.95% in the example). This loop keeps as an offset the adjusted torque level from step 4, preventing large step changes in torque. The torque applied by the turbine will gradually rise, causing the speed to rise slowly and the loop to apply a proportional torque term in proportion to the speed error.
6. When the speed increases up to nearly-exactly-synchronous, switch the control loop over to a PID loop on the phase error (the error signal will be measured and provided by the synchronizing equipment). Whatever torque was commanded just before the switch to the PID phase loop is carried over as an offset in the PID loop (this can be considered an initial integrator windup).
7. When the phase is within acceptable limits (typically 10 degrees), switch quickly from the VFD to the grid. Turn off the VFD, and then close the generator contactor.

The figure below shows the overall speed profile during the last stage of synchronization. The initial steep slope is the period where a constant 8 N-m of starting torque is applied. The flatter slope starting at 2087 seconds is a result of the change in torque to stop the acceleration and the speed loop being applied (at 99.95% of synchronous speed, or 4570 rad/sec). The phase angle loop starts at just after 2089.5 seconds. The dip in speed is a result of the operation of the phase angle loop to bring the phase error down close to zero. The simulation time step for both this and the following figures is 0.1 seconds.

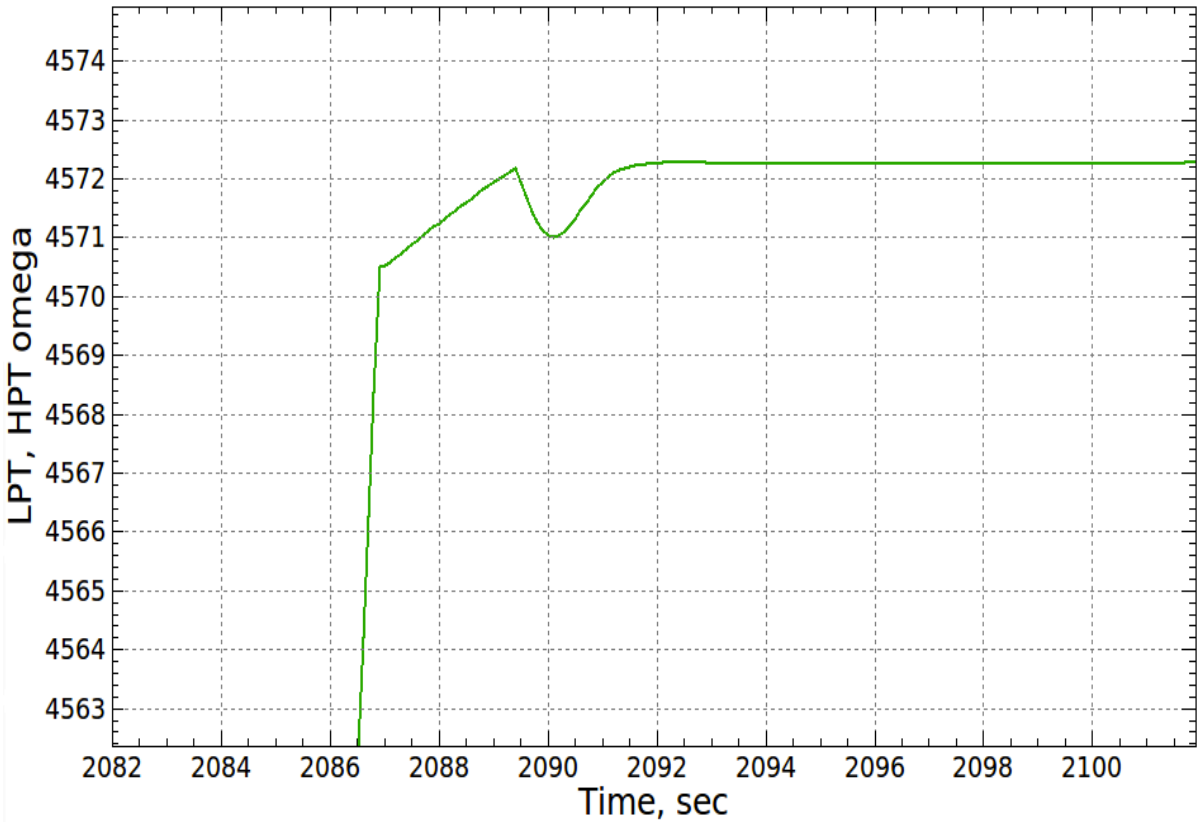

Speed detail during a synchronizing event.

The figure below shows the time history of the synchronization event in which the initial phase error is 1.5 radians mechanical (172^{o} electrical), which represents nearly the worst-case initial phase error. On the plot, the time axis starts at zero when the speed loop starts at step 5 above (when the speed is at or greater than 99.95% of synchronous speed). It is seen that closing the phase error to less than 10^{o} electrical can be achieved in about 5 seconds from the start of the process.

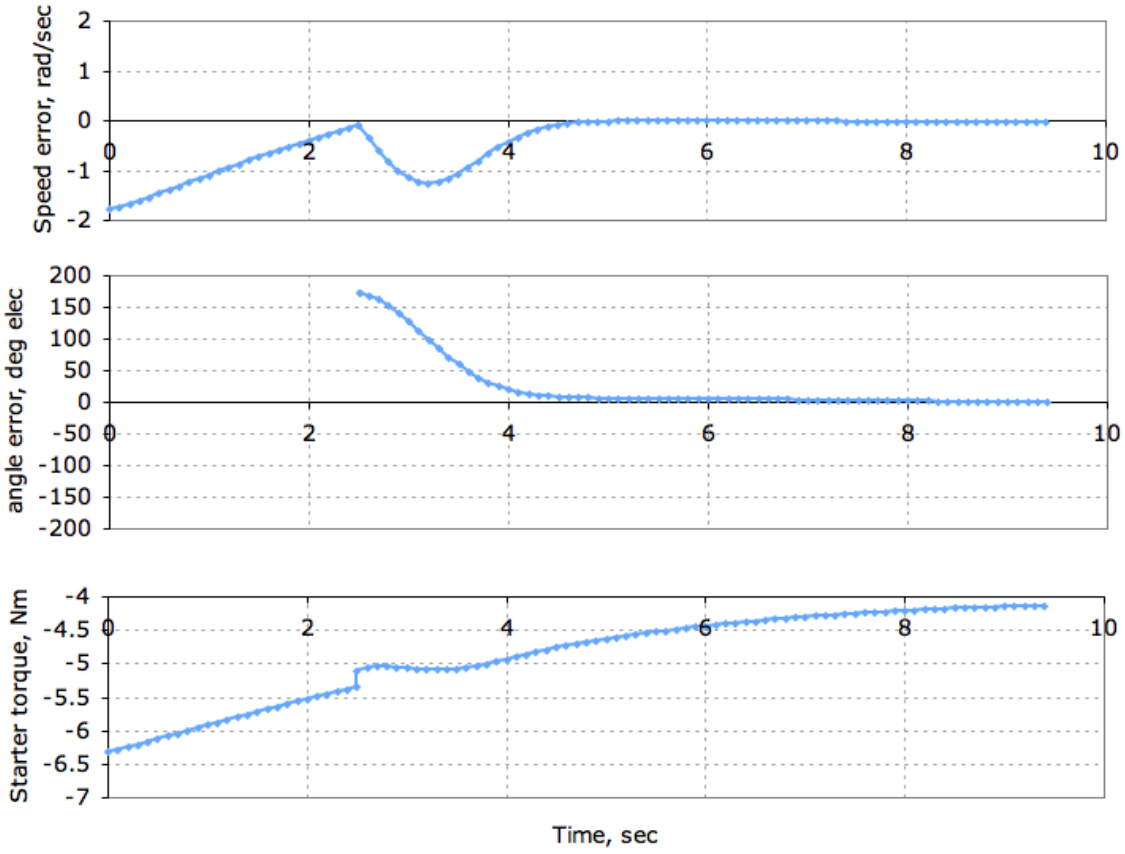

Synchronization with initial phase error of 1.5 radians mechanical (172 deg electrical).

Full Day Simulations

The results from running the dynamic engine simulation for full days of DNI data are shown in the following graphs.

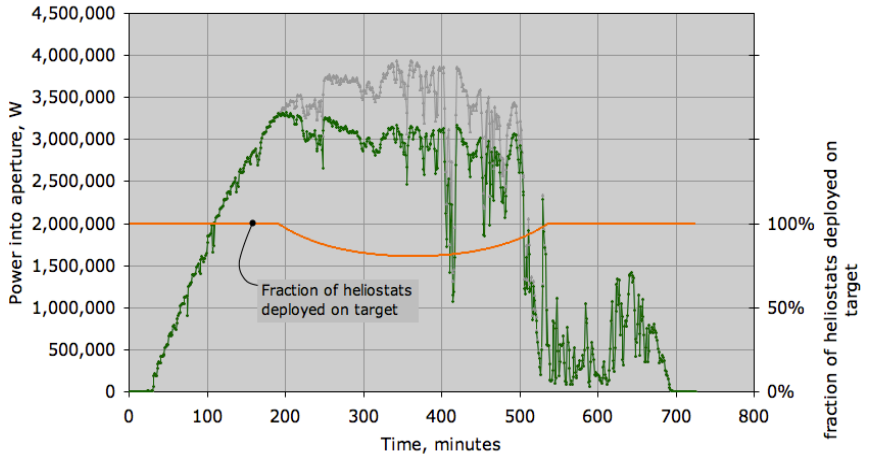

Full day of solar DNI data. Reduction of targeted heliostats in middle of the day is due to de-focussing some of the heliostats when the full-sun DNI produces more power than the engine can use.

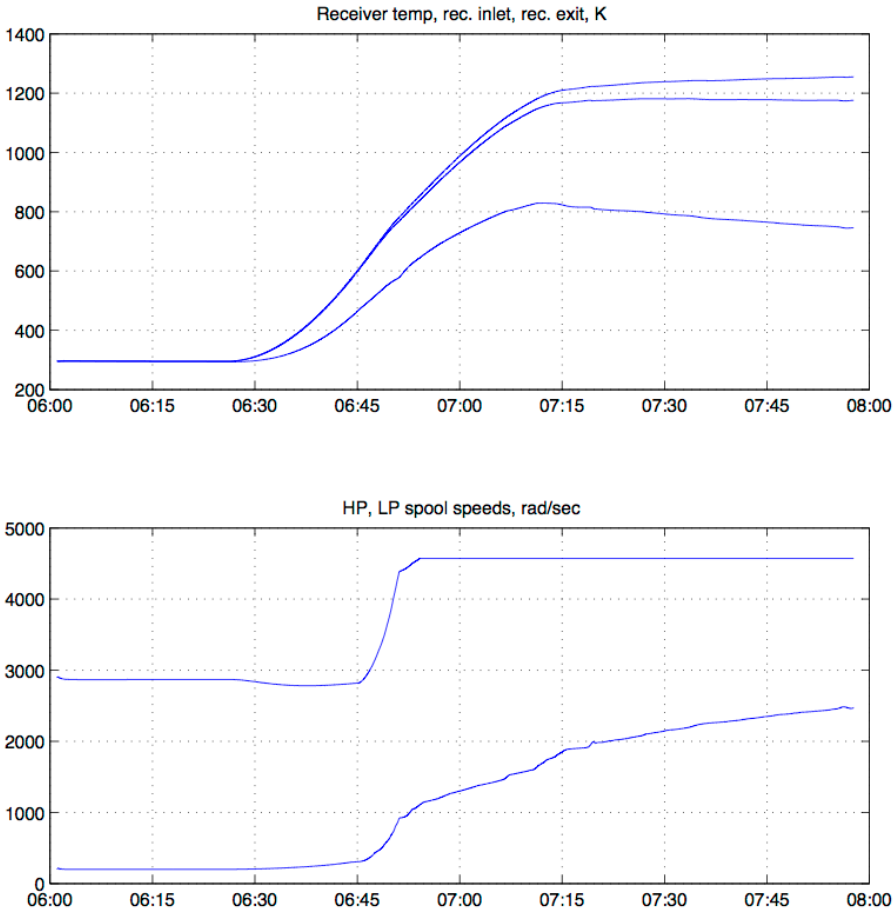

Details of temperature and speed during startup. The time from first light on target to the generator connecting to the grid is about 28 minutes, due to the thermal inertia of the receiver, engine, and supporting hot structures.

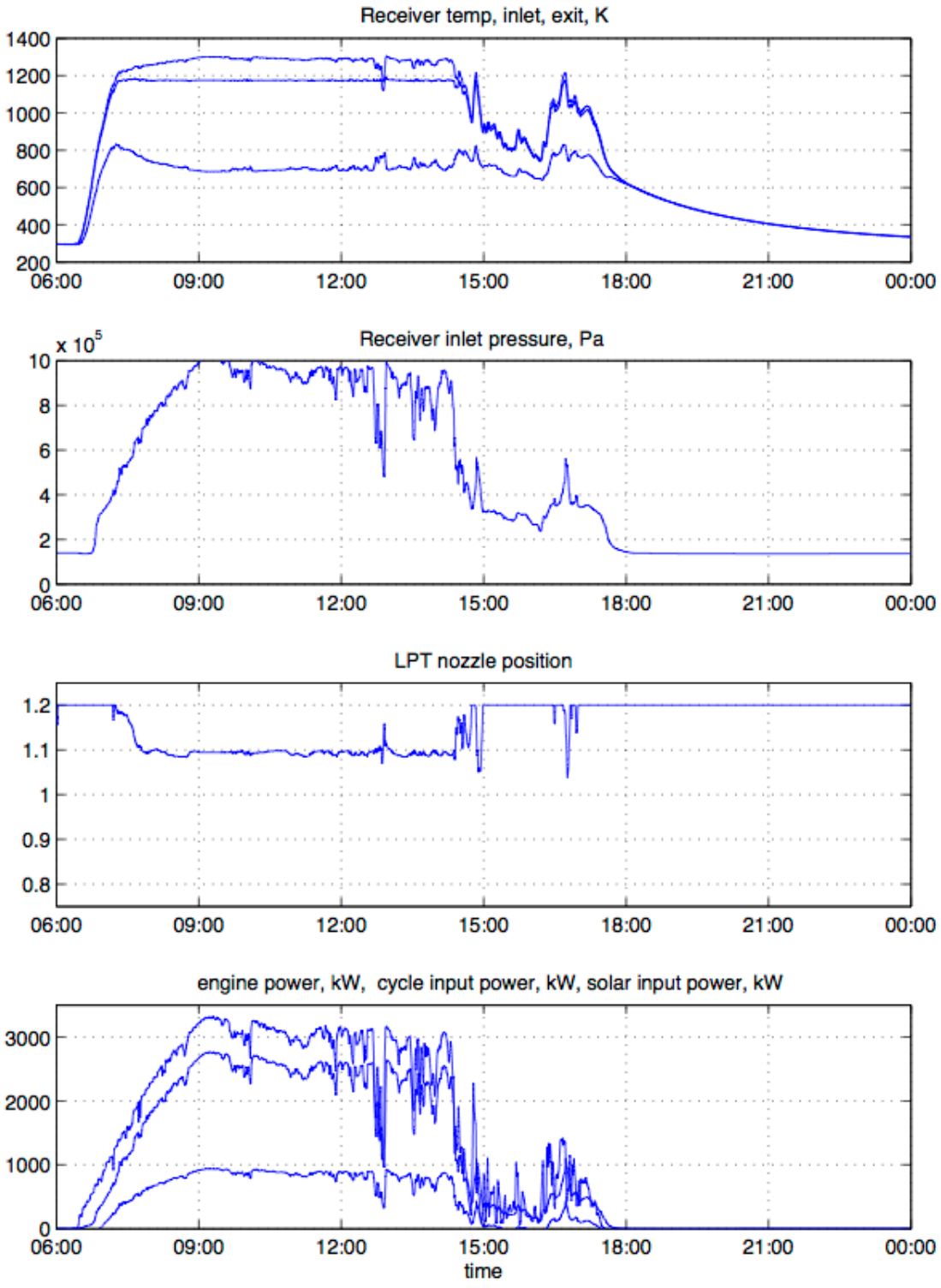

Results from modeling DNI data for a day with volatile solar conditions

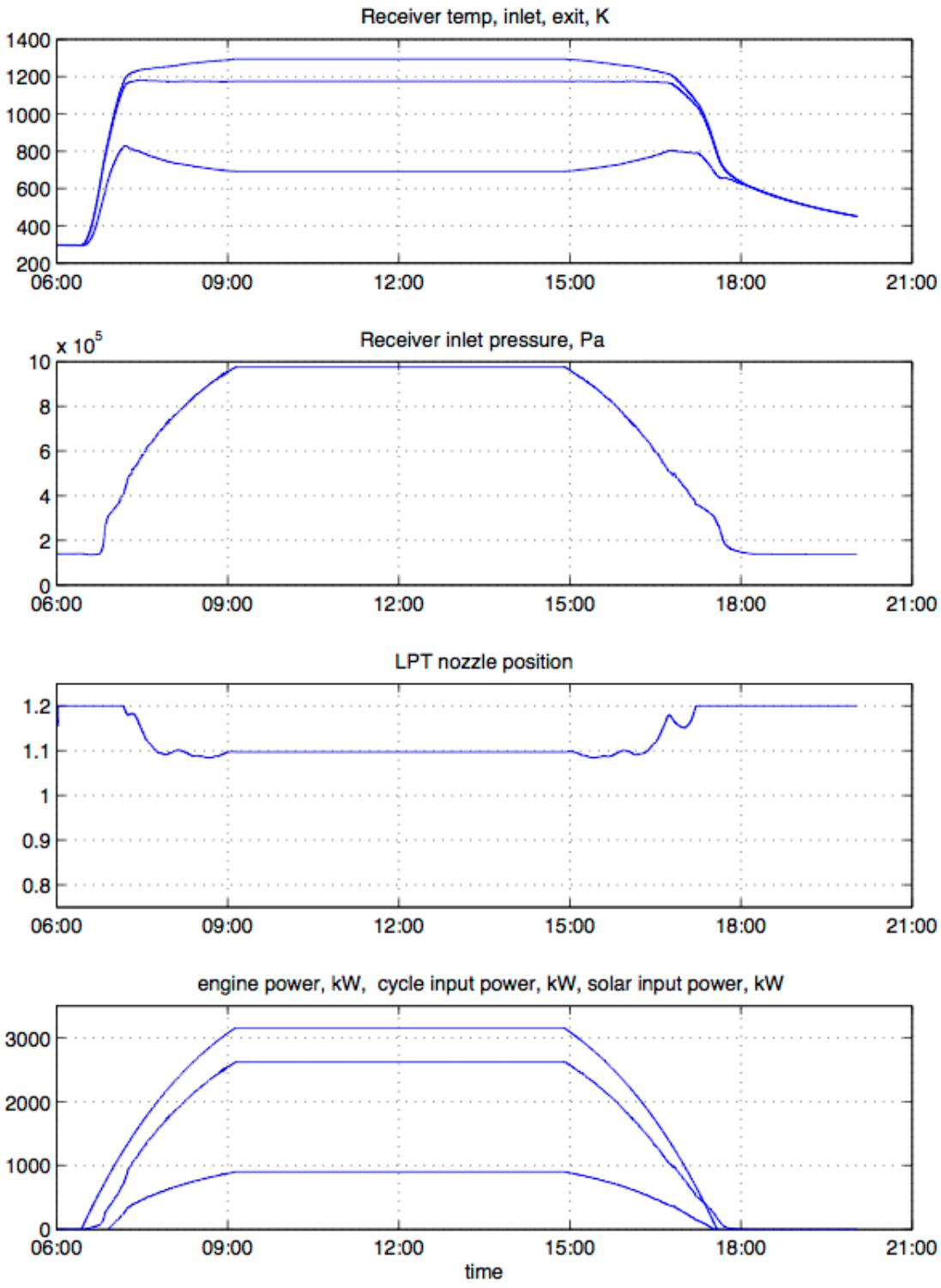

Results from an idealized “cloudless” day

Conclusions

Although we did not ultimately carry out our design through to a prototype, we came away with a number of important results and perspectives on designing and operating a CSP Brayton engine:

- A two-spool Brayton engine with a synchronous generator on a high pressure spool and variable nozzles on a low pressure free spool is capable of stable operation, even with intermittent solar thermal input.
- The engine is expected to be able to continue operation through most cloud transients, but these transients could still impart harmful thermal and stress cycles on the receiver, and need to be managed appropriately.
- Even without fine control over “fuel” input, a solar Brayton engine can be started and synchronized with the electric grid in a robust manner.